

Magnetic and electrical properties of a cyanide-bridged CoCu_3 cluster featuring square pyramidal Cu(II) centers

Yang-Lu Zhang,^a Meng-Tan Cai,^a Yi Chen,^a Fu-Xing Shen,^{b*} Jiong Yang,^{c, d} Junlun Zhu^a and Dong Shao^{a*}

^a *Huber Key Laboratory of Processing and Application of Catalytic Materials, Huber Provincial Engineering Research Center of High Purity Raw Material Processing Technology of Electronic Materials, College of Chemistry and Chemical Engineering, Huanggang Normal University, Huanggang 438000, China*

^b *Institute of Zhejiang University-Quzhou, Quzhou 324000, China*

^c *Department of Physics, Southern University of Science and Technology, Shenzhen 518055, China*

^d *Quantum Science Center of Guangdong-Hong Kong-Macao Greater Bay Area, Shenzhen-Hong Kong International Science and Technology Park, Guangdong 518000, China*

Correspondence and requests for materials should be addressed to
Email: shaodong@nju.edu.cn

Table of Contents

EXPERIMENTAL SECTION.....	3
Figure S1. The complete molecule unit of 1	6
Table S1. Continuous Shape Measure (CShM) analysis for Cu(II) and Co(III) ions in 1	7
Table S2. Selected bond lengths (Å) for 1	8
Table S3. Selected bond angles [°] for 1	9
Table S4. The possible hydrogen bonds in 1 calculated by PLATON.....	10
Figure S2. Highly H-bonded 3D network of 1 viewed along [111] direction.	11
Figure S3. Frequency dependence of the in-phase (χ') and out-of-phase (χ'') part of the ac susceptibilities measured under zero dc field for 1	12
Figure S4. Temperature dependence of the in-phase (χ') and out-of-phase (χ'') part of the ac susceptibilities measured under 1.5 kOe dc fields for 1	12
Figure S5. Cole-Cole plots of 1 . The solid lines represent the best fits according to the generalized Debye model.	13
Table S6. Relaxation fitting parameters from the least-square fitting of the Cole-Cole plots of 1 according to the generalized Debye model.....	13
Table S7. The conductivity of 1 during heating and cooling variable temperature process under 95% RH.....	14
Figure S6. PXRD spectra before and after impedance measurement condition for 1	14
Figure S7. Comparison of the experimental PXRD pattern of 1 with the simulated pattern from its single crystal structure.	15
Figure S8. TGA curve of 1	15
References	16

EXPERIMENTAL SECTION

Physical measurements

Elemental analyses of C, H, and N were performed at an Elementar Vario MICRO analyzer. Infrared spectra were obtained in the range of 600–4000 cm^{−1} on a Bruker tensor II spectrometer. Powder X-ray diffraction data (PXRD) was recorded on a Bruker D8 Advance diffractometer with Cu K α X-ray source ($\lambda = 1.54056$ Å) operated at 40 kV and 40 mA between 5 and 30° (2 θ). Thermal gravimetric analysis (TGA) was carried out on freshly filtered crystals using the Mettler Toledo TGA2 instrument in an insert Ar₂ atmosphere over a temperature range of 27–700 °C with a heating rate of 10 °C/min. Direct current (dc) magnetic susceptibility from 2 to 300 K with applied 1000 Oe dc field were performed using a Quantum Design SQUID VSM magnetometer on the crushed single crystals sample of **1**. Alternative current (ac) magnetic susceptibility data were collected in the temperature range of 2-8 K, under an ac field of 2 Oe, oscillating at frequencies in the range of 1-1000 Hz. All magnetic data were corrected for the diamagnetic contributions of the sample holder and of core diamagnetism of the sample using Pascal's constants.

Proton conductivity

Proton conductivity was characterized through a two-probe method using an electrochemical workstation (DH7007). The test cells containing the pellets were suspended in a commercial temperature and humidity control chamber (DHTHM-27-0-P-SD). Before conductivity measurements, sample was placed in a steel mold and pressed into pellets of 8 mm diameter and 1.2 mm thickness using a tablet press. Data were collected in the frequency range of 1 Hz to 1 MHz and an AC amplitude of 100

mV, thermally equilibrated for 5 hours at each temperature. The resistance values were obtained by fitting the impedance profile using Zview software. Proton conductivity (σ) is estimated by the following equation,

$$\sigma = L / A \cdot R \quad (1),$$

where L and A are the thickness and area of the pellet and R is the bulk resistance estimated by the Nyquist plot. Activation energy of proton conduction (E_a) is estimated by the following equation,

$$\sigma T = \sigma_0 \exp(E_a / kBT) \quad (2),$$

where σ is the proton conductivity, σ_0 is the preexponential factor, k_B is the Boltzmann constant, and T is the temperature.

X-ray Crystallography

Single crystal X-ray diffraction data were collected on a Bruker D8 QUEST diffractometer with a PHOTON III area detector (Mo-K α radiation, $\lambda = 0.71073 \text{ \AA}$, Bruker *IuS* 3.0) at different temperatures controlled by Oxford Cryosystems low-temperature device. The APEX III program was used to determine the unit cell parameters and for data collection. The data were integrated and corrected for Lorentz and polarization effects using SAINT.^{S1} Absorption corrections were applied with SADABS.^{S2} The structures were solved by direct methods and refined by full-matrix least-squares method on $F2$ using the SHELXTL^{S3} crystallographic software package integrated in Olex2.^{S4} All the non-hydrogen atoms were refined anisotropically. Hydrogen atoms of the organic ligands were refined as riding on the corresponding non-hydrogen atoms. Additional details of the data collections and structural

refinement parameters are provided in Table 1. Selected bond lengths and angles of 1 are listed in Table S2, S3. CCDC numbers 2473824 are the supplementary crystallographic data for this paper. They can be obtained freely from the Cambridge Crystallographic Data Centre via www.ccdc.cam.ac.uk/data_request/cif.

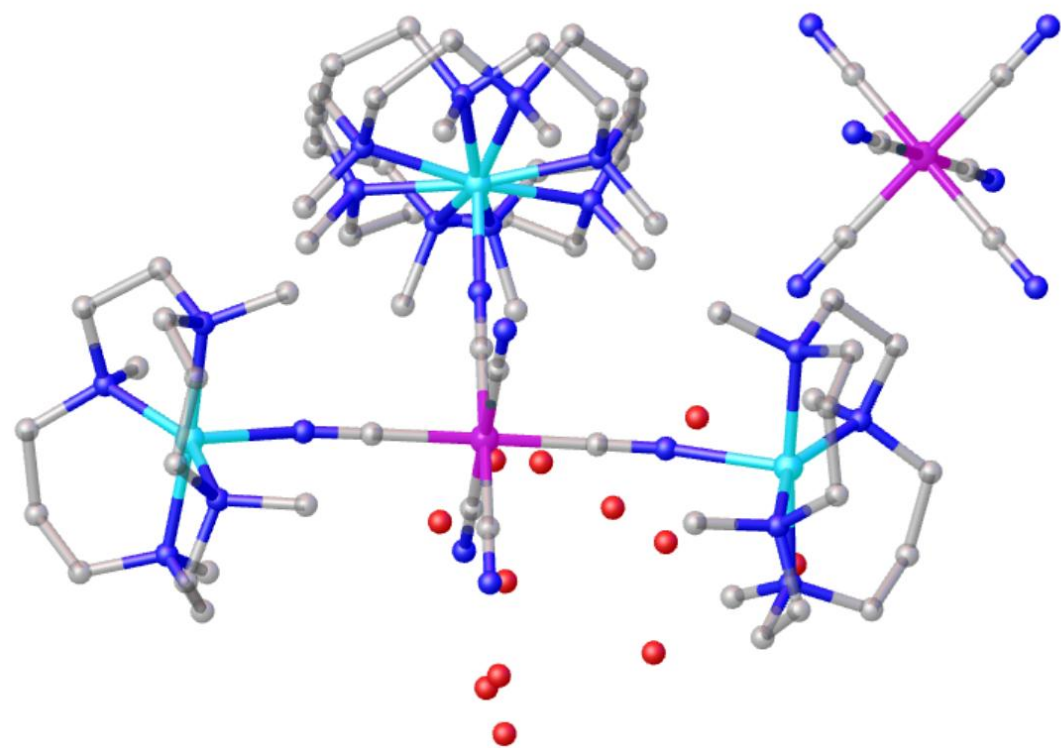


Figure S1. The complete molecule unit of **1**.

Table S1. Continuous Shape Measure (CShM) analysis for Cu(II) and Co(III) ions in 1.

Compound, Metal center	CShM parameters*					Determined coordination geometry
	six-coordinated coordination sphere					
	HP-6	PPY-6	OC-6	TPR-6	JPPY-6	
Co1	33.193	29.957	0.009	16.392	33.559	OC-6
Co2	32.862	30.175	0.006	16.546	33.710	OC-6
	five-coordinated coordination sphere					
	PP-5	vOC-5	TBPY-5	SPY-5	JTBPY-5	
Cu1	27.326	4.144	6.792	3.111	10.045	SPY-5
Cu2	31.743	1.763	2.285	1.306	4.705	SPY-5
Cu1*	27.326	4.144	6.792	3.111	10.045	SPY-5

CShM parameters for six-coordinated complexes:

HP-6 the parameter related to the hexagon (D_{6h})
 PPY-6 the parameter related to the pentagonal pyramid (C_{5v})
 OC-6 the parameter related to the octahedron (O_h)
 TPR-6 the parameter related to the trigonal prism (D_{3h})
 JPPY-6 the parameter related to the Johnson pentagonal pyramid ($C5v$)
 PP-5 Pentagon
 vOC-5 the parameter related to the Vacant octahedron‡ (Johnson square pyramid, J1)
 TBPY-5 the parameter related to the Trigonal bipyramidal
 SPY-5 the parameter related to the Square pyramid
 JTBPY-5 the parameter related to the Johnson trigonal bipyramidal

Table S2. Selected bond lengths (Å) for **1**.

parameter	Value / Å
Cu1-N1	2.127(4)
Cu1-N12	2.090(4)
Cu1-N9	2.119(4)
Cu1-N10	2.077(4)
Cu1-N11	2.103(4)
Cu1-N _{avg.}	2.103
Cu2-N1	2.128(6)
Cu2-N14	2.072(11)
Cu2-N15	2.120(13)
Cu2-N16	2.067(10)
Cu2-N13	2.068(13)
Cu2-N _{avg.}	2.091
Co2-C7	1.909(4)
Co2-C7 ¹	1.909(4)
Co2-C6	1.904(5)
Co2-C6 ¹	1.904(5)
Co2-C8 ¹	1.906(5)
Co2-C8	1.906(5)
Co1-C1 ²	1.878(4)
Co1-C1	1.878(4)
Co1-C4	1.894(8)
Co1-C2	1.880(7)
Co1-C5	1.885(7)
Co-C _{avg.}	1.896
Symmetry transformations used to generate equivalent atoms:	
¹ 2-X,1-Y,1-Z; ² +X,3/2-Y,+Z	

Table S3. Selected bond angles [°] for **1**.

parameter	Value / °
N12-Cu1-N1	102.94(16)
N12-Cu1-N9	93.30(18)
N12-Cu1-N11	85.42(18)
N9-Cu1-N1	92.69(16)
N10-Cu1-N1	107.30(16)
C7-Co2-C7 ¹	180.0
C8 ² -Co1-C8	180.0
C1 ² -Co1-C1	179.7(3)
C2-Co1-C4	178.0(3)
C5-Co1-C3 ²	179.3(4)
C1-N1-Cu1	159.6(4)
C2-N2-Cu2	176.5(6)
Symmetry transformations used to generate equivalent atoms:	
¹ 2-X,1-Y,1-Z; ² +X,3/2-Y,+Z	

Table S4. The possible hydrogen bonds in **1** calculated by PLATON.

D-H...A	d(D- H)	d(H...A)	d(D...A)	<(DHA)
O(1)-H(1A)...N(4)	0.85	2.09	2.8917	158
O(1)-H(1B)...O7	0.85	2.36	3.1687	159
O(3A)-H(2AA)...N(5)	0.85	2.28	3.1230	170
O(3A)-H(2AB)...O(5)	0.85	2.02	2.8688	172
O(5)-H(5A)...N(8)	0.85	2.12	2.8409	142
O(6)-H(6A)...O(3A)	0.85	1.87	2.6917	162
O(7)-H(7A)...O(6)	0.85	2.16	2.8327	135
O(7)-H(7B)...O(5)	0.85	1.95	2.7840	167
N(8)-H(8A)...O(7)	0.85	2.07	2.8222	147
N(8)-H(8B)...N(7)	0.85	1.97	2.8045	167
C(014)-H(01C)...N(1)	0.96	2.06	2.8956	167
C(9)-H(9C)...N(1)	0.96	2.59	3.0319	108
C(21)-H(21A)...O(8)	0.97	2.58	3.4967	157
C(32)-H(32C)...N(3)	0.96	2.62	3.0437	107

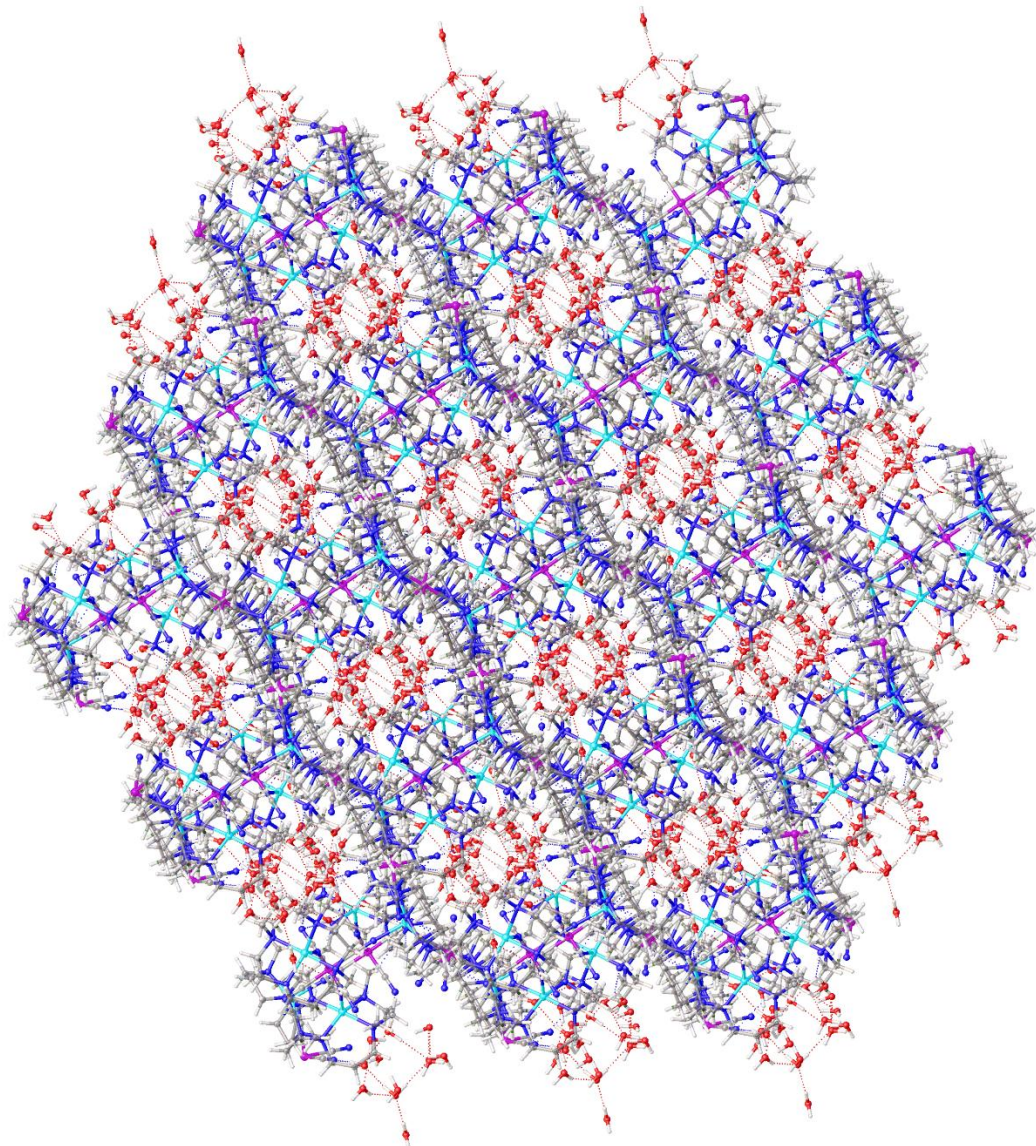


Figure S2. Highly H-bonded 3D network of **1** viewed along [111] direction.

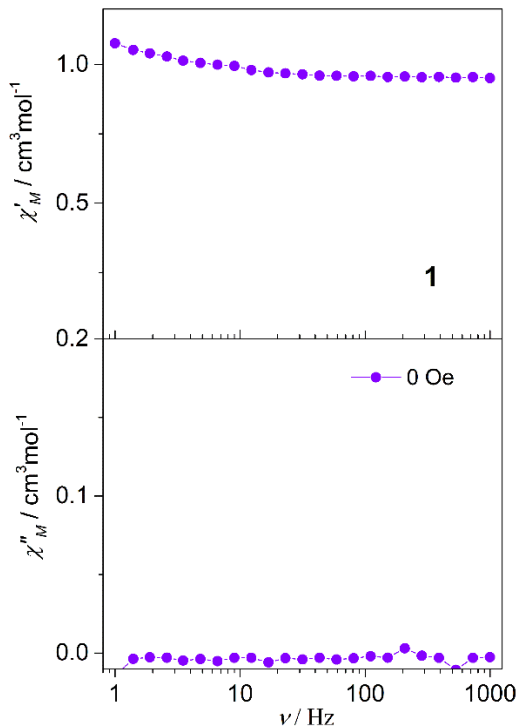


Figure S3. Frequency dependence of the in-phase (χ') and out-of-phase (χ'') part of the ac susceptibilities measured under zero dc field for **1**.

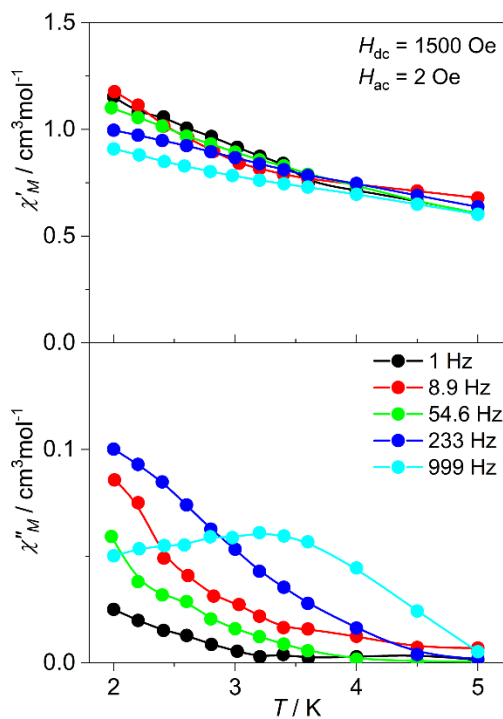


Figure S4. Temperature dependence of the in-phase (χ') and out-of-phase (χ'') part of the ac susceptibilities measured under 1.5 kOe dc fields for **1**.

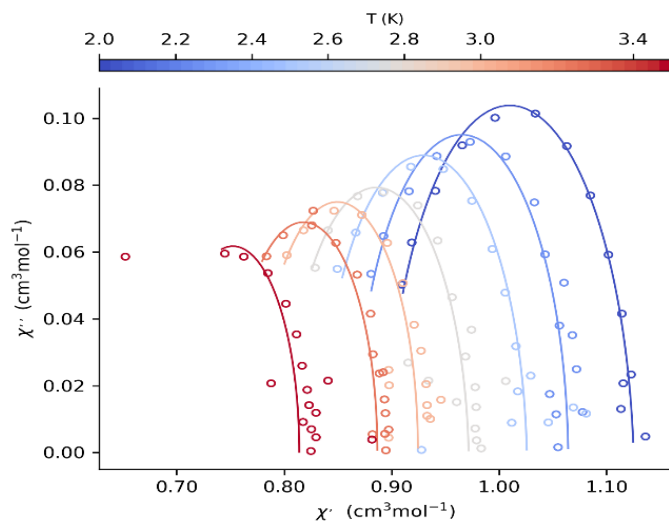


Figure S5. Cole-Cole plots of **1**. The solid lines represent the best fits according to the generalized Debye model.

Table S6. Relaxation fitting parameters from the least-square fitting of the Cole-Cole plots of **1** according to the generalized Debye model.

T / K	τ / s	χ_s / $\text{cm}^3\text{mol}^{-1}\text{K}$	χ_T / $\text{cm}^3\text{mol}^{-1}\text{K}$	α
1.99952	7.74499E-4	0.89449	1.1252	0.06691
2.20019	6.1814E-4	0.86604	1.06433	0.0267
2.40044	5.41043E-4	0.83344	1.02586	0.05028
2.60025	4.24987E-4	0.80007	0.97172	0.05012
2.80156	3.50924E-4	0.77459	0.9245	0.07844
2.99988	2.9859E-4	0.74893	0.88674	0.01697
3.39976	1.88588E-4	0.69056	0.81404	0.00365

Table S7. The conductivity of **1** during heating and cooling variable temperature process under 95% RH.

$T / ^\circ\text{C}$	$\sigma / \text{S cm}^{-1}$	$T / ^\circ\text{C}$	$\sigma / \text{S cm}^{-1}$
25	5.2×10^{-4}	50	5.2×10^{-3}
30	6.9×10^{-4}	45	3.4×10^{-3}
35	8.2×10^{-4}	40	1.2×10^{-3}
40	1.1×10^{-3}	35	8.0×10^{-4}
45	3.6×10^{-3}	30	6.8×10^{-4}
50	5.3×10^{-3}	25	4.9×10^{-4}

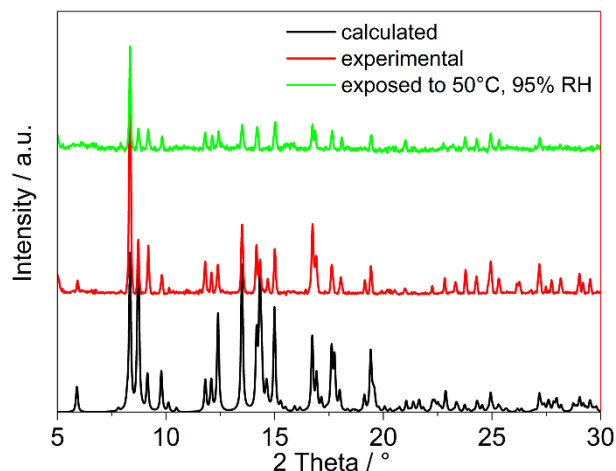


Figure S6. PXRD spectra before and after impedance measurement condition for **1**.

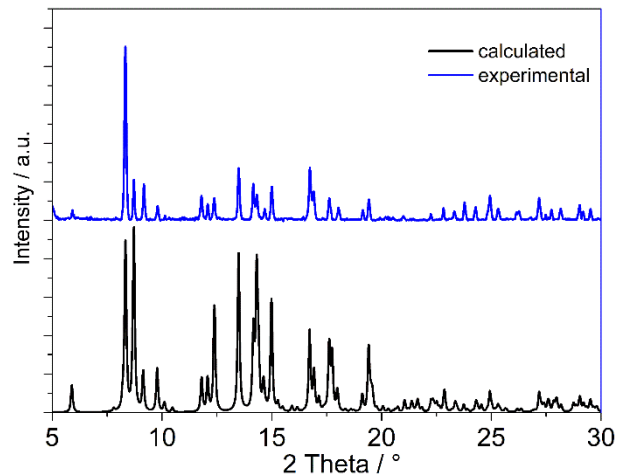


Figure S7. Comparison of the experimental PXRD pattern of **1** with the simulated pattern from its single crystal structure.

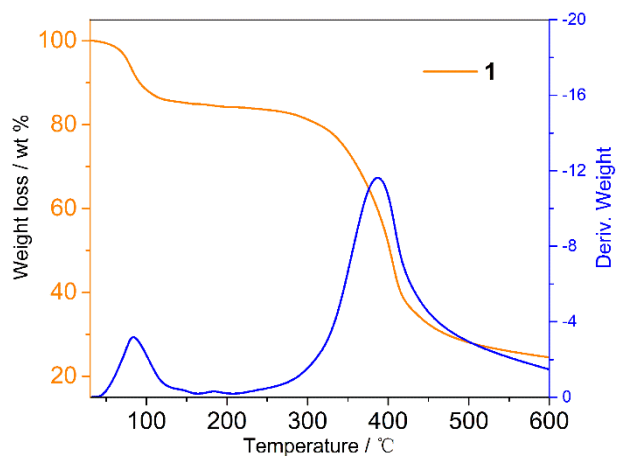


Figure S8. TGA curve of **1**.

References

- S1) SAINT Software Users Guide, version 7.0; Bruker Analytical X-Ray Systems: Madison, WI, 1999.
- S2) G. M. Sheldrick, SADABS, version 2.03; Bruker Analytical X-Ray Systems, Madison, WI, 2000.
- S3) G. M. Sheldrick, SHELXTL, Version 6.14, Bruker AXS, Inc.; Madison, WI 2000-2003.
- S4) Dolomanov, O. V.; Bourhis, L. J.; Gildea, R. J.; Howard, J. A. K.; Puschmann, H. OLEX2: A Complete Structure Solution, Refinement and Analysis Program. *J. Appl. Crystallogr.*, **2009**, 42, 339–341.
- S5) M. Llunell, D. Casanova, J. Cirera, P. Alemany and S. Alvarez, SHAPE, version 2.1, Universitat de Barcelona, 2013.